NONDESTRUCTIVE TESTING USING STRESS WAVES:

WAVE PROPAGATION IN LAYERED MEDIA

A Senior Honors Thesis

by

JOSE ALBERTO ORTEGA

Submitted to the Office of Honors Program
& Academic Scholarships
Texas A&M University
in partial fulfillment of the requirement of the

UNIVERSITY UNDERGRADUATE
RESEARCH FELLOWS

April 2002

Group: Engineering

NONDESTRUCTIVE TESTING USI   'S:

WAVE PROPAGATION IN LA

A Senior Honors The:
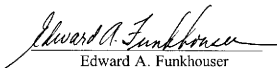
by $5 26$-C

JOSE ALBERTO ORTI   /0

Submitted to the Office of Honors Program
& Academic Scholarships
Texas A&M University
in partial fulfillment of the designation of

UNIVERSITY UNDERGRADUATE
RESEARCH FELLOW

Approved as to style and content by:

_____   _____
José M. Roesset   Edward A. Funkhouser
(Fellows Advisor)   (Executive Director)

April 2002

Group: Engineering

ABSTRACT

Nondestructive Testing Using Stress Waves:

Wave Propagation in Layered Media. (April 2002)

José Alberto Ortega
Department of Civil Engineering
Texas A&M University
Fellows Advisor: Dr. José M. Roesset
Department of Civil Engineering

The use of stress waves in several civil engineering applications such as nondestructive testing of soil deposits or pavement systems has become extremely popular over the last few years. In all cases, a dynamic impulse is applied to the surface of the investigated medium, and the corresponding motions associated with the propagation of stress waves are recorded by receivers located at different points away from the source of loading. In many applications, these are primarily surface (*Rayleigh*) waves. The properties of the medium and the potential existence of defects can be determined from the appropriate interpretation of the recorded motions. Although current interpretation processes are performed considering accurate solutions to the dynamic problem, a situation of interest arises when a soil stratum is underlain by a much stiffer material.

Researchers have established that no surface waves will propagate through a soil medium below a *threshold frequency* for the case when the soil base is assumed to be infinitely rigid. When dealing with vertical loads, some researchers had originally

suggested that the threshold frequency corresponds to the natural frequency of the soil layer in dilatation/compression. This would imply that for a saturated soil having a value of Poisson's Ratio close to 0.5, surface waves would never be generated - a conjecture which is clearly incorrect.

The goals of the research project were to determine the threshold frequency as a function of Poisson's Ratio of the soil layer and to investigate the surface-wave propagation phenomena for values close to the mentioned frequency. Two approaches were utilized to achieve the research objectives. The first approach consisted in developing analytical expressions for the relations between displacements and stresses due to plane waves propagating in a soil layer. The second approach considered the study of the phase shift in the motions at different points under steady state conditions. Both approaches used wave propagation results provided by computer simulation programs.

The results of this study are figures showing the variation of the apparent wave propagation velocity corresponding to the threshold frequency divided by the shear wave velocity of the medium as a function of Poisson's ratio and a comparison with the P-wave velocity.

ACKNOWLEDGEMENTS

TABLE OF CONTENTS

LIST OF FIGURES

CHAPTER I

INTRODUCTION

The use of stress waves in nondestructive testing of laboratory specimens, structural members, pavements systems, and soil deposits has become extremely popular. In all these cases, a dynamic impulse is applied by one or more sources, and the corresponding motions (accelerations, velocities, or displacements) are recorded as functions of time by a series of receivers placed at different points or stations. The properties of the medium or the potential existence of defects such as cracks, inclusions, or cavities are then determined from an appropriate interpretation of the amplitudes of the recorded motions, the times of arrival of the waves at the receivers, inter-arrival times between receivers, or phase differences between the motions at the receivers.

Most of the methods used to interpret the mentioned data and obtain the desired properties were originally based on highly simplified models using ray path theory or assuming a simple type of waves (Nazarian, 1984). These methods were normally acceptable for relatively simple situations, but could not provide the desired accuracy for more complicated and realistic conditions. As a result, more accurate, yet more complex formulations have been developed and implemented over the last few years (Shao 1985, Foinquinos 1995).

This thesis follows the style and format of the *Journal of Structural Engineering*.

The decision that must be made in practice is in some cases between speed (important when having to interpret large amounts of data in a reasonable amount of time) and accuracy (important when dealing with unusual or irregular cases), although with the continuous increase in speed of computation, the use of simplistic methods of analysis is less justifiable. This work looks at some specific cases of nondestructive testing using stress waves to clarify some remaining issues.

The following sections of this chapter will describe concepts related to wave propagation in layered media, nondestructive testing techniques, how they operate, and the interpretation process of their outcomes.

Wave Propagation in Layered Media

The *Spectral Analysis of Surface Waves* (SASW) method is a technique developed over the last twenty years to determine the properties of soil deposits in situ and their variation with depth (Nazarian, 1984). The SASW is a non-intrusive, nondestructive technique, which has been successfully used in practice in a variety of in-land applications, and has been proposed to determine the properties of the subsoil in the ocean floor.

The basis of the SASW method is the application of an impulse load on the free surface of the soil deposit, recording the resulting motions as functions of time at least at two receivers located on the surface as well (Figure 1). The distance spacing between receivers is typically the same as the distance from the source to the first receiver;
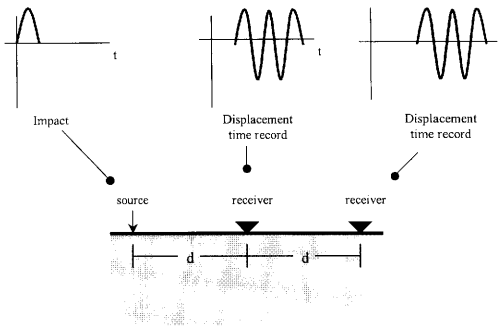
Figure 1. Diagram of the Set Up of a SASW Experiment

subsequently, these distances are changed for each range of frequencies of interest (and their corresponding wavelengths). A number of studies have shown that those distances should be between half and four wavelengths. Generally, the test consists of various load applications for different source and receiver spacings. For a particular spacing, the impact is applied by the source and the motions are recorded at the two receivers. The time records of the displacements obtained at the two receivers are automatically converted to the frequency domain by applying a Fourier transform and obtaining their Fourier spectra with a spectral analyzer.

The mentioned process is equivalent to consider the motions as consisting of a superposition of many sine waves with different frequencies and phases. One can then obtain the phases corresponding to each frequency component. From the phase

difference, one can obtain the inter-arrival time of the waves (difference between the times of arrival at the two receivers), and therefore, their velocity of propagation in the horizontal direction. This kind of velocity is referred to as *phase velocity*. The ratio of the frequency ω to the phase velocity c is the wave number k.

$$k = \frac{\omega}{c} \tag{1}$$

The wavelength is:

$$\lambda = \frac{2\pi}{k} \tag{2}$$

The derivative of ω with respect to k is the group velocity:

$$c_G = \frac{d\omega}{dk} \tag{3}$$

The variation of the phase velocity with frequency or wavelength (computed directly from the other previous two) is called the *dispersion curve*. The process is repeated for each position of source and receivers (Figure 2) five to ten times, and the corresponding results are averaged. The resulting dispersion curve is considered valid over the range of wavelengths corresponding to one-quarter of the receivers spacing and twice this distance. The positions of the receivers are then changed, and the process is repeated (with another five to ten impacts) to obtain a dispersion curve valid over a different range of frequencies (or wavelengths). The ranges of validity of the results for two consecutive sets of tests will normally overlap and will not be identical.
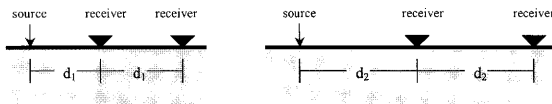
Figure 2. Diagram of the Setup of the SASW Experiment for
Two Different Experiments

The final experimental dispersion curve is formed as a composite of those obtained
from different spacing arrangements. These partial results are smoothed for clearer
visualization of the dispersion curve (Figure 3).

Interpretation of Nondestructive Tests Results

The interpretation of the experimental dispersion curves necessary to compute soil
properties and their variation with depth is based on assumptions that the motions are
caused by surface (*Rayleigh*) waves propagating horizontally from the source to the
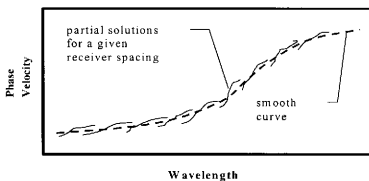
Figure 3. Typical Compound Dispersion Curve for a Soil Deposit
whose Properties Increase with Depth

receiver. For impacts of very short duration, associated with high frequencies, small wavelengths, and short distances from source to first receiver and between receivers, the apparent velocity of propagation of the waves would be controlled by the properties of the soil layer closest to the surface such as the shear modulus, Poisson's ratio, and the soil's density. The Rayleigh wave velocity of this soil stratum can be then obtained directly from the experimental dispersion curve at very high frequencies.

Increasing the duration of the impact will result in lower-frequency waves. The corresponding waves will have longer wavelengths and will penetrate deeper into the soil (Figure 4). Their apparent velocity of propagation will depend on the average properties of the soil over a thicker layer. By knowing the properties of the top layer from the results for a higher frequency, one can obtain those of a second soil layer to have the desired phase velocity for the combination of the two. The process can be
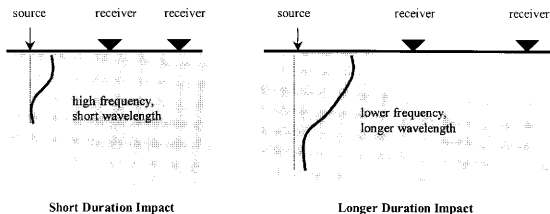
Figure 4. Effect of Increasing the Duration of the Impact Load

continued by sequentially looking at the results for increasingly longer wavelengths (smaller frequencies), and then computing the properties of a bottom soil layer knowing those of the strata above it.

CHAPTER II

RESEARCH PROBLEM

Nondestructive Testing of Soils

Following the process of interpretation of nondestructive tests' results mentioned in the previous chapter, computation of the elastic properties of the soil near the surface is relatively easy. The computation becomes increasingly more cumbersome as the depth at which properties are desired increases. The maximum depth is limited by the ability to produce an impact of sufficient duration and amplitude to produce reliable recordings at large distances. When trying to determine soil properties at great depths, the test often ceases to be nondestructive, relying on dropping large masses from sufficient heights to produce the desired impact duration and magnitude.

The interpretation of the experimental data (dispersion curve) was initially carried out based on some very simple assumptions, considering a simple Rayleigh wave corresponding to the first mode of vibration of the soil. This approach produced reasonable (although not too accurate) results for simple soil profiles, where the properties increased smoothly and gradually with depth. For cases with a stiffer layer near the surface (case of a pavement system, Figure 5), this approach can yield serious errors.
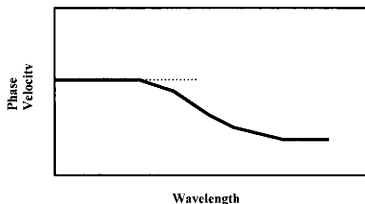
Figure 5. Typical Dispersion Curve for a Pavement System

Today, the interpretation (also called *inversion*) of the data is normally performed considering a more accurate solution of the actual dynamic problem including all types of waves (response of a layered soil deposit to a dynamic load applied at its surface). A number of studies have been carried out to show the difference between the results obtained with this more accurate formulation and those of the more traditional one accounting only for one mode of the theoretical Rayleigh wave (or more properly generalized Rayleigh wave) (Shao 1985, Foinquinos 1995). A situation of interest arises when a soil stratum is underlain by a much stiffer, rock-like material with a sharp transition in elastic properties (Chang, et. al. 1991).

In the limiting case, when the base is assumed to be infinitely rigid, no surface wave will propagate horizontally through the soil below a threshold frequency (Foinquinos, 1995). When applying horizontal (shear) forces on the surface of the soil, this threshold frequency is the natural frequency of the soil deposit in shear:

$$f_{1s} = \frac{c_s}{4H} \tag{4}$$

where: H = thickness of the stratum, C_s = shear wave velocity. The situation is more complicated when dealing with vertical loads as in the case of the SASW test. Some initial studies had suggested that in this case, the threshold frequency would be the natural frequency of the soil layer in dilatation/compression:

$$f_{1p} = \frac{c_p}{4H} \tag{5}$$

where: H = thickness of the stratum, C_p = P wave velocity of the material, given by

$$c_p = c_s \sqrt{\frac{2(1-\upsilon)}{1-2\upsilon}} \tag{6}$$

This is an approximation for values of Poisson's ratio less than one third. In the limits, for a saturated soil with a Poisson's ratio very close to 0.5 the P wave velocity tends to infinity, suggesting that surface waves would never be generated. This last statement is clearly incorrect.

The objective of this research is to find the threshold frequency at which wave propagation occurs for a soil stratum over rigid rock subjected to vertical loads. This can also be considered as the resonant frequency of the stratum under vertical excitation.

Dynamic Stiffness of Foundations

In the design of foundations for large vibrating machines that rotate at a fixed velocity, it is important to know the stiffness of the foundation and the surrounding soil as a function of frequency. This problem is closely related to the previously discussed one with harmonic forces (rather than a transient pulse) being applied on the soil deposit through the foundation. The foundation stiffness as a function of frequency is the

relation between the applied force and the resulting displacement. For the dynamic case, the displacement will be characterized by an amplitude and a phase (representing the phase difference between the force and the displacement). It is common to write the dynamic stiffness of a foundation in the form

$$K_d = K_{st}(k_1 + ia_0 c_1)$$ (7)

where:

K_d is the dynamic stiffness.

K_{st} is the static stiffness = F / W, where F is the static force and W the corresponding static displacement.

k_1, c_1 are dynamic stiffness coefficients, functions of frequency. k_1 represents inertia effects in the soil due to the dynamic loads. c_1 represents the loss of energy by radiation of waves away from the foundation.

a_0 is a dimensionless frequency, $a_0 = \omega \cdot R / c_s$ where ω is the frequency in radians/sec, R is the radius of a circular mat foundation (an equivalent radius for other cases), and c_s is the shear wave velocity of the soil.

The product $K_{st} = R \cdot c_1 / c_s$ can be interpreted as the constant of an equivalent viscous dashpot. The term c_1 is particularly important in assessing the dynamic response of a machine foundation or of a structure subjected to dynamic loads (wind, waves, earthquake) because it can represent a substantial amount of beneficial damping. This damping would considerably reduce the response and is particularly large under vertical vibrations. Unfortunately, c_1 and the corresponding damping would be zero below the threshold frequency for a soil stratum over rigid rock because no waves would propagate

horizontally. In the preliminary stages of the dynamic or seismic design of a structure for which soil-structure interaction effects may be important, it is necessary to know whether one can rely on radiation damping or not. This implies the knowledge of the predominant frequencies of the structure and of the excitation, and of the threshold frequency of the soil deposit.

CHAPTER III

RESEARCH METHODS

The objective of this research project was to develop a better understating of how waves propagate in a soil layer of finite thickness, underlain by a stiffer material, when subjected to dynamic vertical loads applied at its surface. Particularly, this study looked at the frequency at which surface waves could propagate through the soil layer. This was referred to as the *threshold frequency*.

The work started with a review of the basic literature on wave propagation in a half space due to dynamic vertical loads applied at the surface. This is often known as Lamb's problem (Lamb, 1904). Fundamental solutions for pulse and harmonic loads have been developed by a number of authors (Quinlan 1953, Miller and Pursey 1954, Pekeris 1955, Mooney 1974, Holzlohner 1980). The more general numerical solutions for a soil layer or a layered half space were proposed by Apsel (1979) using a continuous formulation and by Kausel (1981) using a discrete formulation. These two approaches have been implemented in special purpose computer programs by Roesset.

Two approaches were then used in this study. The first one is referred to as general wave propagation considerations and consists in developing analytical expressions for the displacements and stresses due to plane wave propagation in a layer. The second considers steady state vibrations of a soil layer under a harmonic load applied at the surface. In this case we look both at the amplitude of the resulting displacements to

assess the frequency at which the peak displacement occurs, and the phase differences between source and receiver or between two receivers.

General Wave Propagation Considerations

Analytical expressions for displacements and stresses due to plane waves propagating through a layer are considered in this section. The objective of developing these expressions was to check the existence of real values for the wave number k for which one can have non-zero motions without any applied forces.

The expression describing the relationship between applied forces and particle displacements is:

$$\begin{bmatrix} t_x \\ t_y \end{bmatrix} = K \cdot \begin{bmatrix} u \\ w \end{bmatrix} \tag{8}$$

where K is the *stiffness matrix* of a soil layer. For the case of in-plane motion:

$$K = \begin{bmatrix} k_{11} & k_{12} \\ k_{21} & k_{22} \end{bmatrix} \tag{9}$$

where k_{11}, k_{12}, k_{21}, and k_{22} are functions of frequency ω and wave number k (or phase velocity c). The expansions of these terms are the following:

$$k_{11} = \frac{kG(1 - S^2)}{sD} \left[C^r S^s - rsC^s S^r \right] \tag{10}$$

$$k_{12} = k_{21} = -\frac{kG(1 - S^2)}{D} \left[1 - C^r C^s + rsS^s S^r \right] - kG(1 + s^2) \tag{11}$$

$$k_{22} = \frac{kG(1 - S^2)}{rD} \left[C^s S^r - rsC^r S^{rs} \right] \tag{12}$$

having:

$$D = 2\left(1 - C^r C^s\right) + \left(\frac{1}{rs} + rs\right) S^r S^s \tag{13}$$

$$r = \sqrt{1 - \left(\frac{\omega}{kc_p}\right)^2} \tag{14}$$

$$s = \sqrt{1 - \left(\frac{\omega}{kc_s}\right)^2} \tag{15}$$

$$C^r = \frac{1}{2}\left(e^{krh} + e^{-krh}\right) \tag{16}$$

$$S^r = \frac{1}{2}\left(e^{krh} - e^{-krh}\right) \tag{17}$$

$$C^s = \frac{1}{2}\left(e^{ksh} + e^{-ksh}\right) \tag{18}$$

$$S^s = \frac{1}{2}\left(e^{ksh} - e^{-ksh}\right) \tag{19}$$

In order to have real values of the wave number k for which non-zero motions exist without any applied loads, one must have the determinant of the stiffness matrix equal to zero, that is:

$$|K| = 0 \tag{20}$$

$$k_{11} k_{22} - k_{12} k_{21} = 0 \tag{21}$$

A Fortran program was implemented to evaluate the determinant of the stiffness matrix and to find values of k or c at which it would become zero. Figure 6 presents some typical dispersion curves, calling:
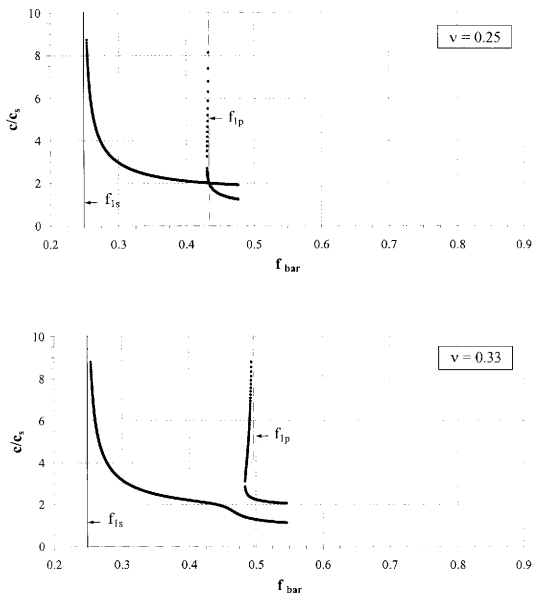
Figure 6. Dispersion Curves for Two Different Values of Poisson's Ratio

$$f_{bar} = \frac{fH}{c_s} \qquad (22)$$

$$\omega_{bar} = 2\pi f_{bar} = \frac{\omega H}{c_s} \qquad (23)$$

where H is the thickness of the soil stratum, c_s is the shear wave velocity of the soil, and v is the value of the Poisson's ratio of the layer.

The determinant of the stiffness matrix K becomes zero among others at the frequencies:

$$f_{bar,ns} = 0.25, 0.75, 1.25 \ldots.$$

$$\omega_{bar,ns} = \pi/2, 3\pi/2, 5\pi/2 \ldots.$$

which are the natural frequencies of the soil stratum in shear and at the frequencies:

$$f_{bar,np} = 0.25 \frac{c_p}{c_s}, 0.75 \frac{c_p}{c_s}, 1.25 \frac{c_p}{c_s} \ldots.$$

$$\omega_{bar,np} = (\pi/2) \frac{c_p}{c_s}, (3\pi/2) \frac{c_p}{c_s}, (5\pi/2) \frac{c_p}{c_s} \ldots.$$

which are the natural frequencies of the soil stratum in compression or dilatation.

At the frequencies $f_{bar,ns}$ the terms k_{11}, k_{12}, k_{21} become zero and the horizontal displacements would become infinity under a horizontal load. At the frequencies $f_{bar,np}$ the vertical displacements would become infinity under vertical loads. Starting at these frequencies we have dispersion curves, providing for each value of ω one or more values of c or k at which the determinant is zero. Figure 6 illustrates these results (only the first two dispersion curves are shown) for values of Poisson's ratio, $v = 0.25$ and 0.45. These studies were repeated for a number of values of Poisson's ratio.

Steady-State Vibrations

Under steady state vibrations due to harmonic vertical loads, one can obtain the amplitudes and the phases of the motions at various receivers (directly under the load or at some distance). Using Fortran programs, which address the solution to the wave propagation phenomena, amplitude and phase angle spectra were developed for several cases. Figured 7 and 8 present examples of the results obtained from this part of the study.
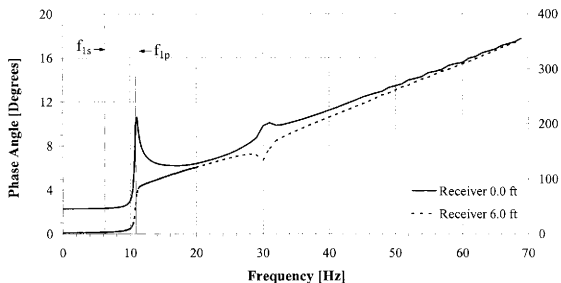

Figure 7. Phase Angle Spectrum for a Layer over a Rigid Base
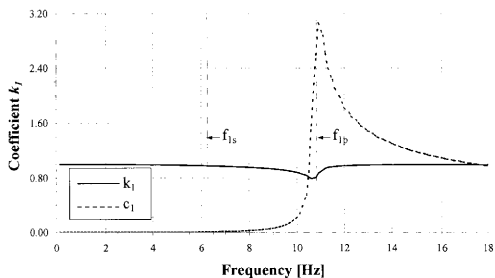($\nu = 0.25$, $H = 20$ ft, $c_s = 500$ ft/s, Radius = 0.5 ft, Damping = 2%)
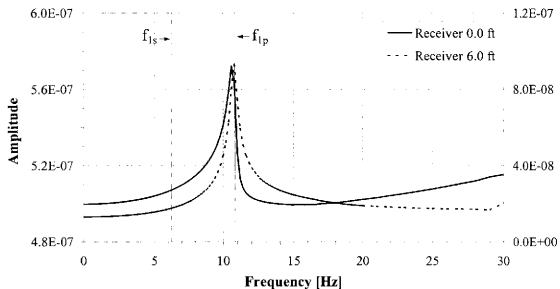
Figure 8. Amplitude Spectrum for a Layer over a Rigid Base
($\nu = 0.25$, $H = 20$ ft, $c_s = 500$ ft/s, Radius = 0.5 ft, Damping = 2%)

Finally figures 9 and 10 show the dynamic stiffness coefficients k_i, c_i for a circular foundation. Figure 9 corresponds to the horizontal stiffness and Figure 10 to the vertical stiffness. It can be seen that the horizontal stiffness coefficient k_i has a dip at the natural frequency of the stratum in shear, while the c_i coefficient is zero below this frequency. In Figure 10, for the vertical stiffness the dip occurs at the frequency corresponding to the frequency of the peak in Figure 8 and the c_i coefficient has a sharp increase around this frequency.
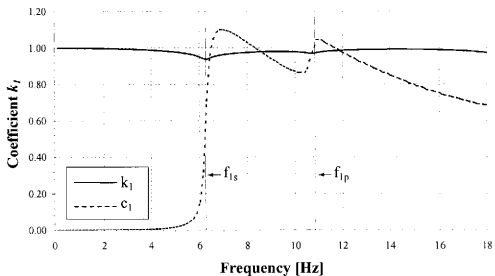
Figure 9. Horizontal Dynamic Stiffness Coefficients for a Circular Foundation
($\nu = 0.25$, $H = 20$ ft, $c_s = 500$ ft/s, Radius = 0.5 ft, Damping = 2%)

Figure 10. Vertical Dynamic Stiffness Coefficients for a Circular Foundation
($\nu = 0.25$, $H = 20$ ft, $c_s = 500$ ft/s, Radius = 0.5 ft, Damping = 2%)

CHAPTER IV

SUMMARY OF RESULTS

General Wave Propagation Approach

Figure 11 presents the dispersion curves showing values of the phase velocity c as function of the dimensionless frequency f_{bar} for which the determinant of the dynamic stiffness matrix of a layer becomes zero. Only the first two dispersion curves are shown. The first one starts at the natural frequency of the soil layer in shear ($f_{s,bar} = 0.25$). At this frequency, the wave number for a zero determinant would be $k = 0$, leading to an infinite phase velocity. As the dimensionless frequency increases the phase velocity decreases and tends to the Rayleigh wave velocity. For values of Poisson's ratio (v) larger than 0.15 the first dispersion curve exhibits a clear oscillation with two inflection points. Figure 12 shows for this dispersion curve the plot of the wave number k versus the dimensionless frequency f_{bar}, while Figure 13 shows the variation of the group velocity over the frequency range with the oscillation. It can be seen that the group velocity has a maximum and a minimum over this range. The value at which the group velocity is minimum has been labeled in this study as f_{th2}.

The second dispersion curve starts at the natural frequency of the soil layer in dilatation/compression, $f_{p,bar} = 0.25 \cdot c_p/c_s$ for low values of Poisson's ratio and has a shape similar to that of the first curve. As Poisson's ratio increases, however, the shape
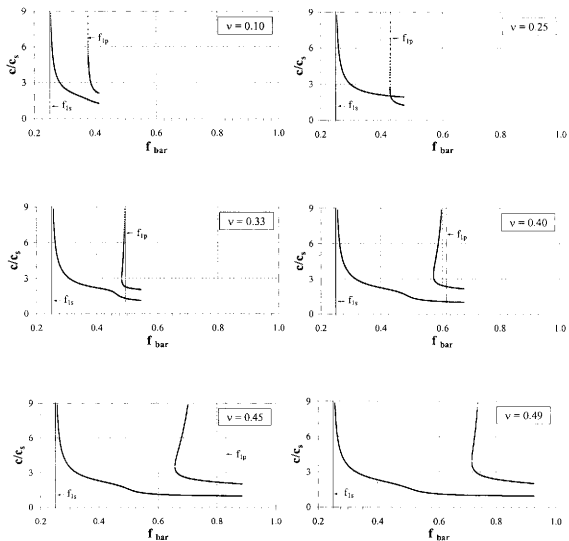
Figure 11. Dispersion Curves of a Layer over a Rigid Base for
Different Values of Poisson's Ratio
($H = 1.0$, $c_s = 1.0$)
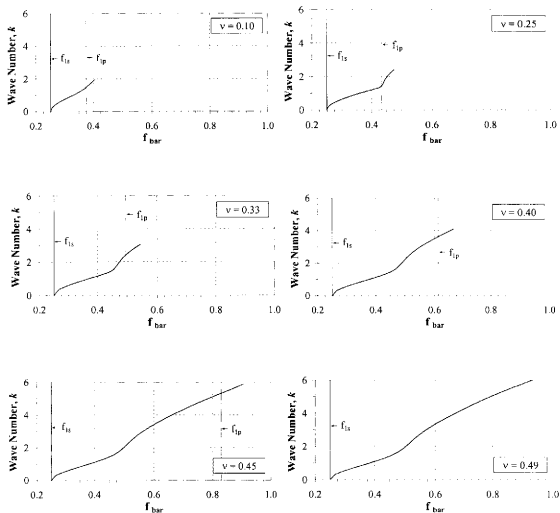
Figure 12. Dispersion Curves of a Layer over a Rigid Base for Different Values of Poisson's Ratio based on the Wave Number k
($H = 1.0$, $c_s = 1.0$)
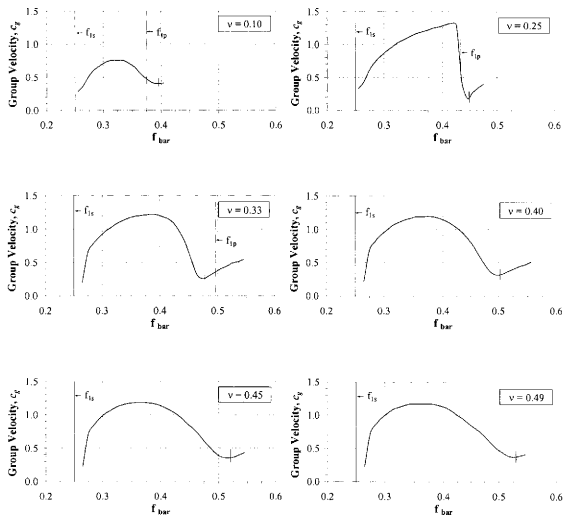
Figure 13. Variation of Group Velocity for Dispersion Curves of a
Layer over a Rigid Base for Different Values of Poisson's Ratio
($H = 1.0$, $c_s = 1.0$)

of this curve changes drastically and has two roots for each frequency for values larger than a minimum frequency f_{th1}.

Figure 14 shows the variation with Poisson's ratio of various frequencies relative to the first natural frequency of the stratum in shear f_s. They are the extension-dilatation natural frequency f_p, the frequency corresponding to the threshold of the second dispersion curve f_{th1}, and the frequency corresponding to the minimum group velocity f_{th2}. In the second part of the study we compare the frequency at which the peak amplitudes of displacement is reached with these two frequencies.
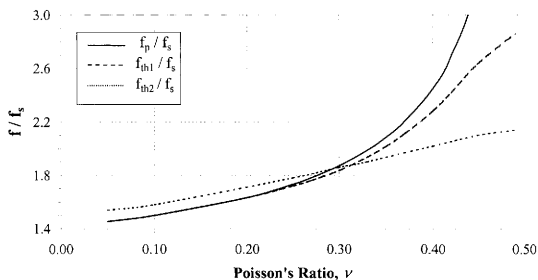
**Figure 14.** Significant Frequencies as Functions of Poisson's Ratio

Steady-State Vibrations

Figures 15, 16, and 17 show the amplitudes and phases of the vertical displacements recorded under the load source and at a distance of 6 ft when a harmonic vertical load is applied on the surface of a soil layer. The layer has a thickness of 20 ft, a shear wave velocity of 500 ft/s, and Poisson's ratio changes from 0.25 (Figure 15) to 0.35 (Figure 16) and 0.45 (Figure 17). The radius of the loaded area is 0.5 ft.

It can be seen that the amplitude reaches a peak at a frequency f_{th}. The phase is essentially zero below this frequency and has a sudden jump around the frequency. As Poisson's ratio increases the frequency of the peak in the amplitude curve seems to increase slightly with increasing distance to the source and the jump in the value of the phase becomes a much smoother one. Additionally, it is observed that the phase starts to grow from the frequency f_{ls} (shear wave natural frequency for the stratum), increasing slowly at first and has then a sharp increase around the frequency f_{th}.

Figures 18, 19, and 20 show on the other hand the dynamic stiffness coefficients k_l and c_l for a rigid circular mat of radius 0.5 ft resting on the surface of the same soil stratum. For values of Poisson's ratio of 0.25 (Figure 18), 0.35 (Figure 19), and 0.45 (Figure 20), the results shown are the stiffness coefficients for horizontal and vertical vibrations.

From these graphs, it is observed that the horizontal stiffness coefficient k_l has a first dip at the natural frequency of the stratum in shear for any value of Poisson's ratio, while
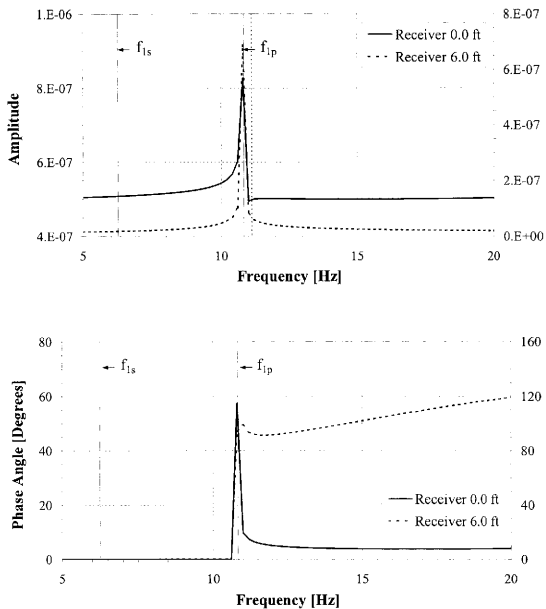
Figure 15. Amplitude and Phase Angle Spectra of a Layer over a Rigid Base
for a Value of Poisson's Ratio, $\nu = 0.25$
($H = 20$ ft, $c_s = 500$ ft/s, Radius = 0.5 ft, Damping = 0%)
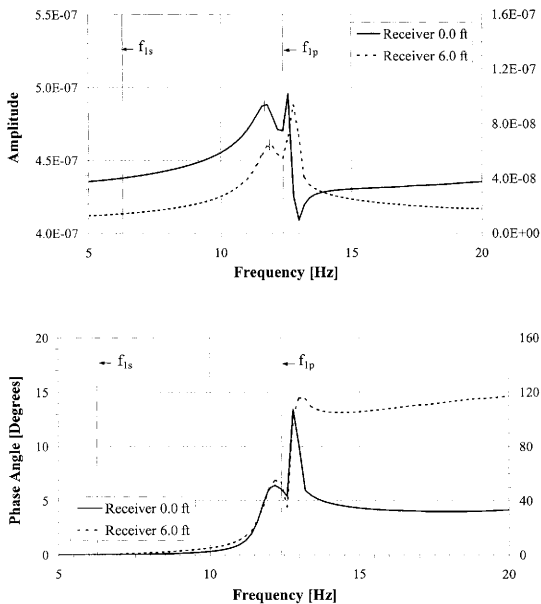
Figure 16. Amplitude and Phase Angle Spectra of a Layer over a Rigid Base for a Value of Poisson's Ratio, $\nu = 0.35$ ($H = 20$ ft, $c_s = 500$ ft/s, Radius $= 0.5$ ft, Damping $= 0\%$)
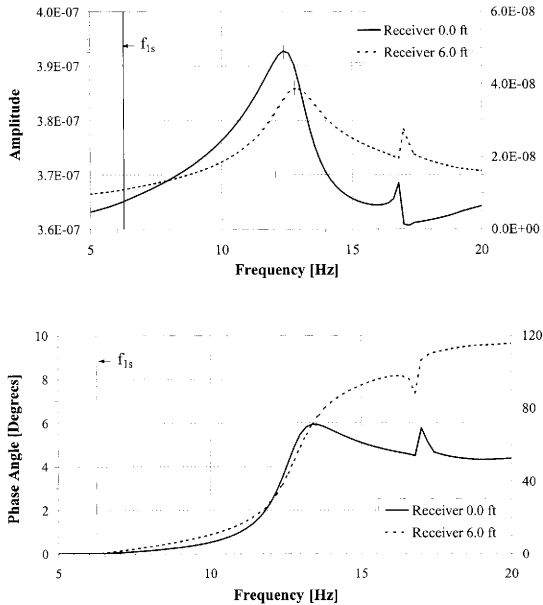
Figure 17. Amplitude and Phase Angle Spectra of a Layer over a Rigid Base for a Value of Poisson's Ratio, $\nu = 0.45$ ($H = 20$ ft, $c_s = 500$ ft/s, Radius = 0.5 ft, Damping = 0%)
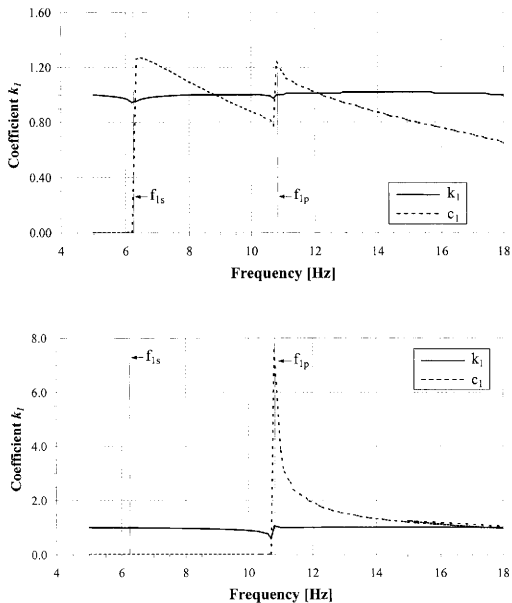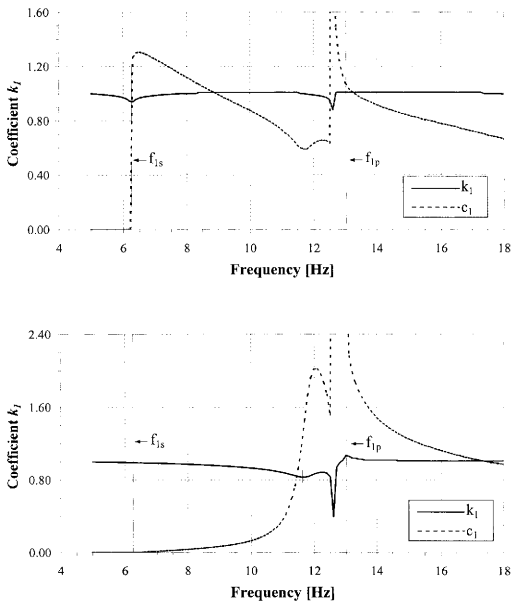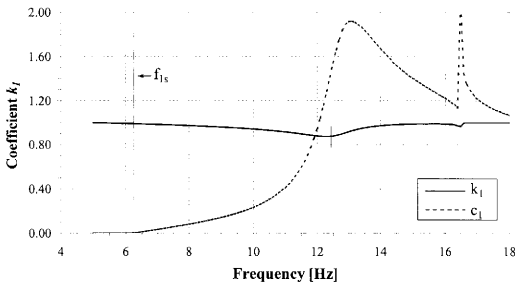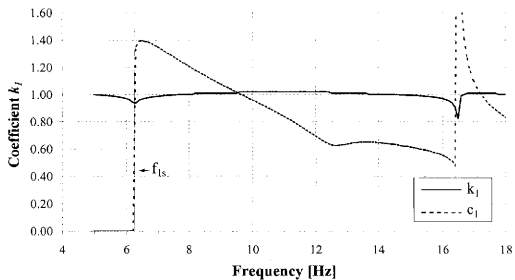
Figure 18. Horizontal and Vertical Dynamic Stiffness Coefficients for a Circular Foundation ($v = 0.25$, $H = 20$ ft, $c_s = 500$ ft/s, Radius = 0.5 ft, Damping = 0%)

Figure 19. Horizontal and Vertical Dynamic Stiffness Coefficients for a Circular Foundation ($\nu = 0.35$, $H = 20$ ft, $c_s = 500$ ft/s, Radius = 0.5 ft, Damping = 0%)

Figure 20. Horizontal and Vertical Dynamic Stiffness Coefficients for a Circular Foundation ($\nu = 0.45$, $H = 20$ ft, $c_s = 500$ ft/s, Radius = 0.5 ft, Damping = 0%)

the c_l coefficient has a value of zero below this frequency. Once this frequency is reached, the c_l coefficient abruptly increases. For the cases of the vertical stiffness coefficients, both dynamic stiffness coefficients remain essentially constant below the natural frequency of the stratum in shear for any value of Poisson's ratio. Subsequently, the k_l coefficient presents the first dip at the frequency f_{th}, while the value of the c_l coefficient increases around this frequency. For small values of Poisson's ratio, the increase of the c_l coefficient is abrupt, while for larger values this increase is gradual. These findings, based on the study of the dynamics of a foundation, agree with the results from the steady-state vibration analysis for a receiver placed underneath the source of loading. Figure 21 shows the variation with Poisson's ratio of the f_{th} frequencies for the two different cases of receiver locations relative the first natural frequency of the stratum in shear.

Finally, Figure 22 presents a summary of the findings of the different approaches used in this study to identify the frequencies at which horizontal wave propagation occurs due to the application of vertical loads on a soil layer underlain by a rigid stratum. The natural frequency of the stratum in dilatation/compression, the frequency corresponding to the threshold of the first dispersion curve (general wave propagation considerations), the frequency corresponding to the minimum group-wave velocity, and the threshold frequencies for the two receiver locations based on the steady-state vibration studies are plotted versus Poisson's ratio.
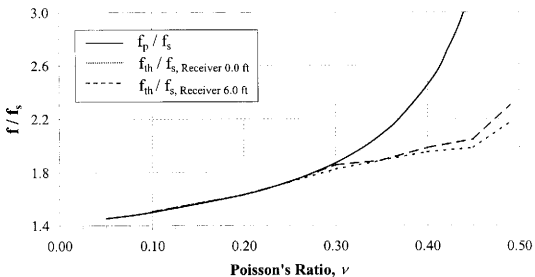
Figure 21. Significant Frequencies as Functions of Poisson's Ratio based on the First Peaks of Amplitude Spectra
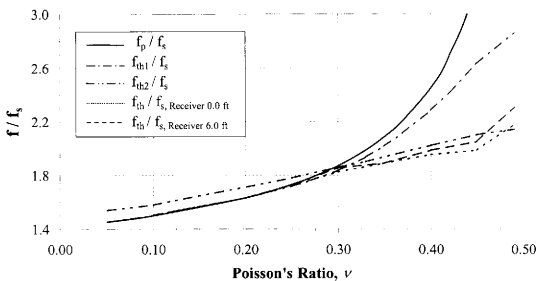
Figure 22. Threshold Frequencies as Functions of Poisson's Ratio

REFERENCES

Apsel, R.J. (1979). "Dynamic Green's functions for Layered Media and Applications to Boundary-Value Problems." Ph.D. Dissertation, University of California at San Diego.

Chang, D.W., Kang, Y.V., Roesset, J.M. and Stokoe, K.H., II. (1991). "Effects of the Bedrock on Profile Backcalculation using the Deflection Measurements of Pavements." Symposium on Nondestructive Deflection Testing and Backcalculation for Pavements, TRB.

Chen, J. F. and Teng, J. G. (2001). "Anchorage Strength Models for FRP and Steel Plates Bonded to Concrete." *Journal of Structural Engineering*, ASCE 127(7), 784-791.

Foinquinos, R. (1995). "Dynamic Nondestructive Testing of Pavements." Ph.D. Dissertation, University of Texas at Austin.

Holzlohner, H. (1980). "Vibrations of the Elastic Half Space due to Vertical Surface Loads." *Earthq. Eng. Struc. Dyn.*, pp. 405-414.

Kausel, E. (1981). "An Explicit Solution for the Green Functions for Dynamic Loads in Layered Media." *Research Report R81-13*, Dept. of Civil Eng., Massachusetts Institute of Technology.

Lamb, H. (1904). "On the Propagation of Tremors over the Surface of an Elastic Solid." *Phil. Tran. Roy. Soc. A*, pp. 1-42.

Miller, G.F. and Pursey, H. (1954). "The Field and Radiation Impedance of Mechanical Radiators of the Free Surface of a Semi-Infinite Isotropic Solid." *Proc. Roy. Soc.,* pp. 521-541.

Mooney, H. (1974). "Some Numerical Solutions for Lamb's Problem." *Bull. Seism. Soc. Am.,* pp. 473-491.

Nazarian, S. (1984). "In Situ Determination of Elastic Moduli of Soil Deposits and Pavement Systems by Spectral-Analysis-of-Surface-Waves Method." Ph.D. Dissertation, The University of Texas at Austin.

Pckeris, C.L. (1955). "The Seismic Surface Pulse." Proc. Natn Acad. Sci. USA, pp.469-480.

Quinlan, P.M. (1953). "The Elastic Theory of Soil Dynamics." ASTM STP 156, *Symposium on Dynamic Testing of Solids*, pp. 3-34.

Shao, K. Y. (1985). "Dynamic Interpretation of Dynaflect, Falling Weight Deflectometer and Spectral Analysis of Surface Waves Tests on Pavement Systems." Ph.D. Dissertation, the University of Texas at Austin.

VITA

José Alberto Ortega was born in Cuenca, Ecuador in September 1978. Son of Dr. Alberto Ortega and Magdalena Andrade de Ortega, he spent his childhood and youth in his home country. After successfully completing his studies at Rafael Borja High School he became a foreign exchange student sponsored by Youth For Understanding. He then spent one year living in San Antonio, TX, opportunity which allowed him to learn about Texas A&M and its undergraduate engineering program. Accepted into the College of Engineering in 1998, he is currently pursuing his Bachelors of Science in Civil Engineering with emphasis on structures and construction management.